Distinct roles of light-activated channels TRP and TRPL in photoreceptors of *Periplaneta americana*

Paulus Saari,[1]* Andrew S. French,[2] Päivi H. Torkkeli,[2] Hongxia Liu,[2] Esa-Ville Immonen,[1,3] and Roman V. Frolov[1]*

[1]Biophysics Group, Nano and Molecular Systems Research Unit, University of Oulu, Oulu FI-90014, Finland
[2]Department of Physiology and Biophysics, Dalhousie University, Halifax, Nova Scotia B3H 4R2, Canada
[3]Lund Vision Group, Department of Biology, Lund University, 223 62 Lund, Sweden

Electrophysiological studies in *Drosophila melanogaster* and *Periplaneta americana* have found that the receptor current in their microvillar photoreceptors is generated by two light-activated cationic channels, TRP (transient receptor potential) and TRPL (TRP-like), each having distinct properties. However, the relative contribution of the two channel types to sensory information coding by photoreceptors remains unclear. We recently showed that, in contrast to the diurnal *Drosophila* in which TRP is the principal phototransduction channel, photoreceptors of the nocturnal *P. americana* strongly depend on TRPL. Here, we perform a functional analysis, using patch-clamp and intracellular recordings, of *P. americana* photoreceptors after RNA interference to knock down TRP (TRPkd) and TRPL (TRPLkd). Several functional properties were changed in both knockdown phenotypes: cell membrane capacitance was reduced 1.7-fold, light sensitivity was greatly reduced, and amplitudes of sustained light-induced currents and voltage responses decreased more than twofold over the entire range of light intensities. The information rate (IR) was tested using a Gaussian white-noise modulated light stimulus and was lower in TRPkd photoreceptors (28 ± 21 bits/s) than in controls (52 ± 13 bits/s) because of high levels of bump noise. In contrast, although signal amplitudes were smaller than in controls, the mean IR of TRPLkd photoreceptors was unchanged at 54 ± 29 bits/s[1] because of proportionally lower noise. We conclude that TRPL channels provide high-gain/high-noise transduction, suitable for vision in dim light, whereas transduction by TRP channels is relatively low-gain/low-noise and allows better information transfer in bright light.

INTRODUCTION

In insect photoreceptors, absorption of a photon by a visual pigment molecule triggers a cascade of biochemical reactions culminating in opening of cationic channels belonging to the TRP (transient receptor potential) superfamily (Hardie, 2014). Until recently, these light-activated channels were identified and studied exclusively in the fruit fly *Drosophila melanogaster*. Its photoreceptors express two channels, TRP and TRPL (TRP-like), characterized by a high degree of similarity with vertebrate TRPC channels (Montell and Rubin, 1989; Hardie and Minke, 1992; Phillips et al., 1992; Niemeyer et al., 1996). Mutant analysis indicated that TRP appears to be the predominant contributor to the total light-induced current (LIC): although the *trp* knockout phenotype was characterized by a global deterioration of photoreceptor function, *trpl* knockout gave only relatively small changes (Hardie and Minke, 1992; Niemeyer et al., 1996; Leung et al., 2000). Because TRPL expression increases substantially in chronically light-deprived flies (Bähner et al., 2002), it was suggested that TRPL might specifically facilitate visual information transfer in dim light, whereas TRP would be important for vision in the well-illuminated habitats of the normally day-active fruit fly. However, testing this hypothesis requires identifying the light-activated channel molecules in species with different visual ecologies and behaviors.

We recently showed that the properties of native LIC in the nocturnal cockroach *Periplaneta americana* closely match those in *trp* knockout *Drosophila*, including large quantum bumps, and their relatively low dependence on extracellular calcium (Immonen et al., 2014b). Subsequent retinal transcriptome analysis yielded the sequences of two putative light-activated channels highly similar to *Drosophila* TRP and TRPL (French et al., 2015). Knockdown of *P. americana* TRP and TRPL channels using RNA interference (RNAi) by injections of long double-stranded RNA (dsRNA) sequences specifically targeting these channels resulted in drastic decreases in their respective mRNA levels and strong changes in electroretinogram (ERG) amplitudes. Importantly, TRP and TRPL mRNA levels were actually increased by about half after the injection of the alternate dsRNA, suggesting the existence of compensatory

*P. Saari and R.V. Frolov contributed equally to this paper.
Correspondence to Roman V. Frolov: roman.frolov@oulu.fi

Abbreviations used: dsRNA, double-stranded RNA; ERG, electroretinogram; GWN, Gaussian white noise; IDR, inactivating delayed rectifier; IR, information rate; Kv, voltage-activated K^+; LIC, light-induced current; MWUT, Mann–Whitney *U* test; RNAi, RNA interference; SNR, signal-to-noise ratio; SROCC, Spearman's rank-order correlation coefficient; TRP, transient receptor potential; TRPkd, TRP knockdown; TRPL, TRP-like; TRPLkd, TRPL knockdown.

The Rockefeller University Press $30.00
J. Gen. Physiol. 2017 Vol. 149 No. 4 455–464
https://doi.org/10.1085/jgp.201611737

mechanisms controlling expression of light-activated channels (French et al., 2015). In preliminary patch-clamp recordings quantum bump amplitudes were reduced fourfold in TRPL knockdown (TRPLkd) but remain largely intact in TRP knockdown (TRPkd) photoreceptors (Immonen et al., 2017).

In the present study, we performed a detailed electrophysiological analysis of *P. americana* TRPkd and TRPLkd photoreceptors created using RNAi. Patch-clamp recordings from dissociated photoreceptors were used to evaluate their basic properties, elementary and macroscopic LIC, and voltage-activated K^+ (Kv) current. Intracellular experiments provided voltage responses to steady and contrast-modulated light stimuli. We show that suppression of TRP or TRPL expression induces profound changes in photoreceptor functions that illustrate the different properties of the two channel types and their probable roles in phototransduction under different illumination conditions.

MATERIALS AND METHODS

Experiments involving *P. americana* (Linnaeus), order Blattodea, were performed in accordance with the Code of Ethics of the World Medical Association (Declaration of Helsinki). American cockroaches were purchased from Blades Biological (Blades Biological Ltd) and maintained in reversed 12–12 illumination conditions with a subjective "night" period matching the actual day. Only male cockroaches were used for experiments.

RNAi

dsRNA was synthesized and injected (4–5 µg in 1 µl Ringer solution) into the head tissue under CO_2 anesthesia as described previously (French et al., 2015; Immonen et al., 2017). In brief, reverse transcription was performed using total RNA extracted from cockroach retinas and oligo $d(T)_{23}VN$ primers with ProtoScript II reverse transcription (New England Biolabs, Inc.). The reverse transcription product was used in PCRs to amplify the template DNAs using Q5 High-Fidelity DNA Polymerase (New England Biolabs, Inc.). dsRNA was synthesized with the MEGAscript RNAi kit (Ambion, Thermo Fisher Scientific). The GenBank accession numbers for *P. americana* TRP and TRPL sequences are KC329816 and KC292630, respectively. The primers and complete dsRNA sequences have been published before (French et al., 2015; Immonen et al., 2017). For injection, a small hole was made in the in chitin of the frontal part of the head below an imaginary line connecting the antennas. Solution was delivered using a sterile disposable glass pipette. After the injection, animals were maintained in separate cages at 25°C. Control animals either received no injection or were injected with 1 µl cockroach Ringer solution.

Patch-clamp recordings

Ommatidia were dissociated and whole-cell recordings were performed as described previously (Frolov, 2015). In brief, data were acquired using an Axopatch 1-D patch-clamp amplifier, Digidata 1550 digitizer, pCLAMP 10 software (Axon Instruments/Molecular Devices). Patch electrodes were made from a thin-walled borosilicate glass (World Precision Instruments) and had resistances in the range from 4 to 9 MΩ. Bath solution contained (mM): 120 NaCl, 5 KCl, 4 $MgCl_2$, 1.5 $CaCl_2$, 10 TES (*N*-Tris-(hydroxymethyl)-methyl-2-amino-ethanesulfonic acid), 25 proline, and 5 alanine, pH 7.15. Patch pipette solution contained (mM): 120 K-glutamate, 20 KCl, 10 TES, 2 $MgCl_2$, 4 Mg-ATP, 0.4 Na-GTP, and 1 NAD, pH 7.15. The liquid junction potential (LJP) was −12 mV. All voltage values cited in the text were corrected for the LJP. The series resistance was compensated by 80%. Membrane capacitance was calculated from the total charge flowing during capacitive transients for voltage steps from −112 to −92/−82 mV. Light stimulation was performed as described previously (Frolov, 2015). Stimulus intensity in patch-clamp and intracellular recording experiments was attenuated with a series of neutral density filters (Kodak). The filters provided up to 11 light intensity backgrounds in 0.5 log unit steps, indicated in Figs. 2 B and 4 C as $\log(I/I_0)$: 0, −0.5, −1,…, −5. The spectral class of photoreceptors was determined using a simple protocol consisting of 20-ms isoquantal flashes of light from all 10 LEDs at an intermediate light intensity. Only green-sensitive photoreceptors, which showed stable resting potential ≤45 mV, identifiable quantum bump responses in the voltage-clamp mode in dim light, and relatively stable electrode-membrane seal properties were used for analysis. Recordings were performed at room temperature (20–22°C) during *P. americana*'s subjective night.

Intracellular recordings

In vivo intracellular single-electrode recordings were performed as described previously (Heimonen et al., 2012). In brief, the dorsal part of the left compound eye was used in the experiments. Photoreceptor responses were recorded using microelectrodes (borosilicate glass; Harvard Apparatus) manufactured with a laser puller (P-2000; Sutter Instrument) and filled with 2 M KCl solution, pH 6.84, to a final resistance of 100–150 MΩ. The reference electrode was placed through the left antenna into the subcutaneous tissue. Signals were recorded with an intracellular amplifier (SEC-05L; NPI). All cells used for analysis had resting potentials of −50 mV or lower and demonstrated transient depolarization with the zero attenuation filter of at least 20 mV in amplitude. For light stimulation, a computer-controlled custom-made voltage-to-current converter was used to drive 13 monochromatic LEDs (Roithner Laser Technik), covering a range from

355 to 625 nm, in combination with neutral density filters (Kodak). All recordings were conducted from green-sensitive photoreceptors at room temperature during the subjective night period.

Data analysis

To determine the information transfer rate, we used a 61-s stimulus consisting of 30 repetitions of a 2-s Gaussian white noise (GWN) sequence, with contrast of 0.36 and a 3-dB cutoff frequency (f_{3dB}) of 50 Hz. The GWN sequence was preceded by an adapting 1-s steady light interval of the same mean intensity to accommodate the initial transient. Data analysis was done in MATLAB (MathWorks) as described previously (Frolov, 2015). In brief, a 2-s signal, $S(f)$, was obtained by averaging voltage responses to 30 repetitions of the 2-s sequence. The noise, $N(f)$, was then obtained by subtracting the signal estimate from the original (noise-containing) sequences and averaging the noise spectra. The contrast gain-of-voltage response, $|T(f)|$, was calculated by dividing the cross-spectrum of photoreceptor input (GWN contrast, $C(f)$) and output (photoreceptor signal, $S(f)\cdot C^*(f)$, where * denotes the complex conjugate), by the autospectrum of the input $C(f)\cdot C^*(f)$ and taking the absolute value of the resulting frequency response function $T(f)$: $T(f) = S(f)\cdot C^*(f)/C(f)\cdot C^*(f)$. The Shannon information rate (IR) was calculated as IR = $\int(\log_2[|S(f)|/|N(f)|+1])\,df$ within a frequency range from 1 to 30 Hz.

Statistics

At the initial stage of statistical analysis, the Shapiro–Wilk normality test was applied to data samples to determine if they could be analyzed using parametric statistical methods. Data in the samples that did not pass the normality test were presented using medians and interquartile ranges (25% quartile:75% quartile). To evaluate differences between such samples, the Mann–Whitney *U* test (MWUT) was used. However, samples that passed the normality test were analyzed with parametric statistical methods as indicated. Such data are presented as mean ± SD and compared using a two-tailed unpaired *t* test with unequal variances. Spearman's rank-order correlation coefficient (SRO CC; ρ) was used in the analysis of correlations. Spearman's ρ was considered significantly different from zero when $P < 0.05$. Throughout the text, *n* indicates sample size.

RESULTS

Elementary responses

Patch-clamp experiments were performed from TRPLkd and TRPkd photoreceptors between days 21 and 35 after injection. Of three basic electrophysiological properties (resting potential, input resistance, and whole-cell capacitance), only capacitance differed significantly from control photoreceptors. Capacitance (C_m) was strongly reduced: 416 ± 137 pF in control (n = 85, the same sample as in Immonen et al. [2017]) versus 243 ± 58 pF in TRPLkd (n = 20; $P < 10^{-6}$, unpaired *t* test) and 247 ± 50 pF in TRPkd (n = 19; $P < 10^{-6}$, unpaired *t* test) photoreceptors.

Consistent with the preliminary results, which were based on smaller experimental groups than those used in this work (Immonen et al., 2017), RNAi caused a dramatic fourfold decrease in quantum bump amplitude in TRPLkd, but not TRPkd, photoreceptors (Fig. 1). Quantum bumps evoked from a holding potential of −82 mV were −41.1 ± 14.8 pA in control (n = 26, the same sample as in Immonen et al. [2017]), −10.3 ± 6.6 pA in TRPLkd (n = 9, $P < 10^{-6}$, unpaired *t* test), and −37.7 ± 24.4 pA in TRPkd (n = 15) photoreceptors. However, in many TRPLkd photoreceptors of otherwise acceptable quality, the quantum bumps were too small to be measured reliably. Therefore, the mean TRPLkd bump amplitude value provided above is likely to be a substantial overestimate.

Absolute sensitivity to light was estimated by counting quantum bumps elicited by steady continuous low-intensity light stimulation evoking <10 bumps per second. As *P. americana* photoreceptors are characterized by large variability in absolute sensitivity, bump rates obtained at different intensity backgrounds with the help of different neutral density filters were recalculated for the common light intensity corresponding to "−5" attenuation level in Fig. 2 B. Absolute sensitivity positively correlated with capacitance in all three groups, although a statistically significant correlation was only found in control photoreceptors, which had the largest number of experiments: SROCC ρ values were 0.76 in control (n = 49, $P < 10^{-6}$), 0.50 in TRPLkd (n = 8, P = 0.18), and 0.37 in TRPkd (n = 15, P = 0.17). Absolute sensitivity was strongly reduced in the knockdown photoreceptors. Its median was 3.9 (1.7:14.5) in control (n = 38), 1.3 (0.3:4.4) in TRPLkd (n = 8), and 0.2 (0.1:1.0) in TRPkd (n = 15); mean values were larger: 8.8 in control, 3.0 in TRPLkd, and 2.4 in TRPkd photoreceptors. However, because of large variability and dependence of absolute sensitivity on capacitance, it was necessary to determine if the differences in sensitivity could be accounted for by the differences in capacitance. For this purpose, a subsample with mean capacitance of 251 pF (n = 12), which is close to the mean C_m values in TRPLkd (253 pF) and TRPkd (247 pF) photoreceptors as presented in Fig. 1 C, was selected from the overall controls, and the corresponding absolute sensitivity values (median 1.7, mean 2.5) were compared with those in the knockdown photoreceptors using the MWUT. No statistically significant differences were found. Although these results imply that compensatory changes in TRPLkd and TRPkd photoreceptors are lim-

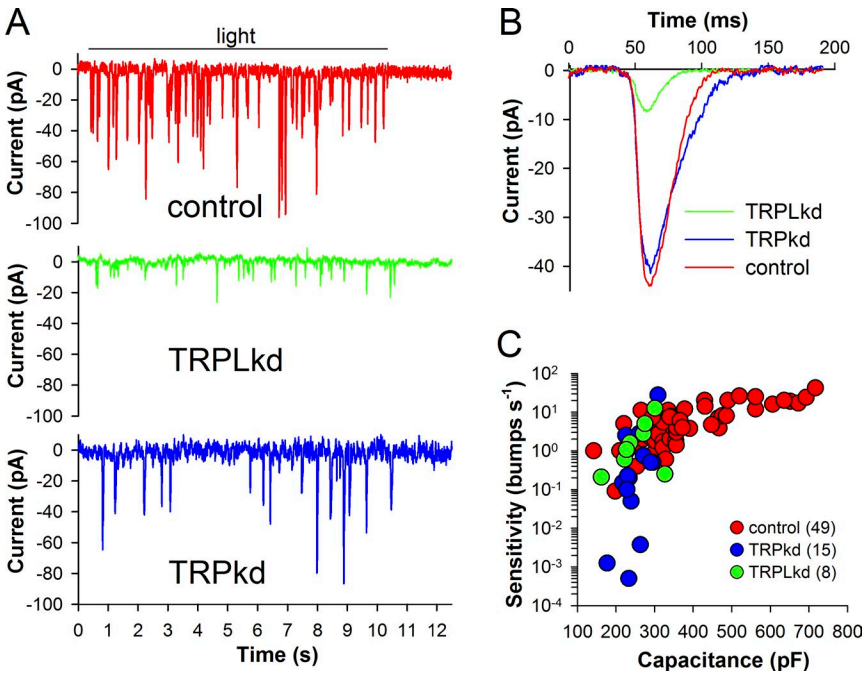

Figure 1. **Quantum bumps and absolute sensitivity to light.** (A) Typical voltage-clamp recordings of quantum bumps elicited by 10-s low-intensity light stimuli from a holding potential of −82 mV in control, TRPLkd, and TRPkd photoreceptors. (B) Mean quantum bumps from traces in panel; means were obtained by aligning rising phases of the bumps. (C) Absolute sensitivity to light was determined by counting bump rates in response to continuous stimulation at light intensities evoking <10 bumps per second; the rates were recalculated for the common level corresponding to the "−5" attenuation level in Fig. 2 B.

ited to the decrease in the number of microvilli (see Discussion), the presence of three outliers with very low absolute sensitivity estimates in TRPkd (Fig. 1 C) invites caution in interpreting these data.

Macroscopic LICs

We estimated LICs in control, TRPkd, and TRPLkd photoreceptors evoked by progressively bright light pulses applied in 10-fold intensity increments, as shown by examples in Fig. 2 A. Despite large cell-to-cell variability in amplitude and time dependence of photoreceptor responses, both knockdown LICs were consistently smaller than control. Notice that recordings from TRPLkd photoreceptors have much smaller bump noise levels than control or TRPkd photoreceptors. Bump noise is caused by variability in quantum bump amplitude and timing.

The dependencies of sustained LIC amplitude (determined 5 s after the onset of light) on stimulus intensity over the entire range of light intensities are shown in Fig. 2 B. Because the amplitude distributions were not Gaussian, the data are presented both as medians with interquartile ranges (circles with error bars) and as means (solid lines). Statistical tests performed

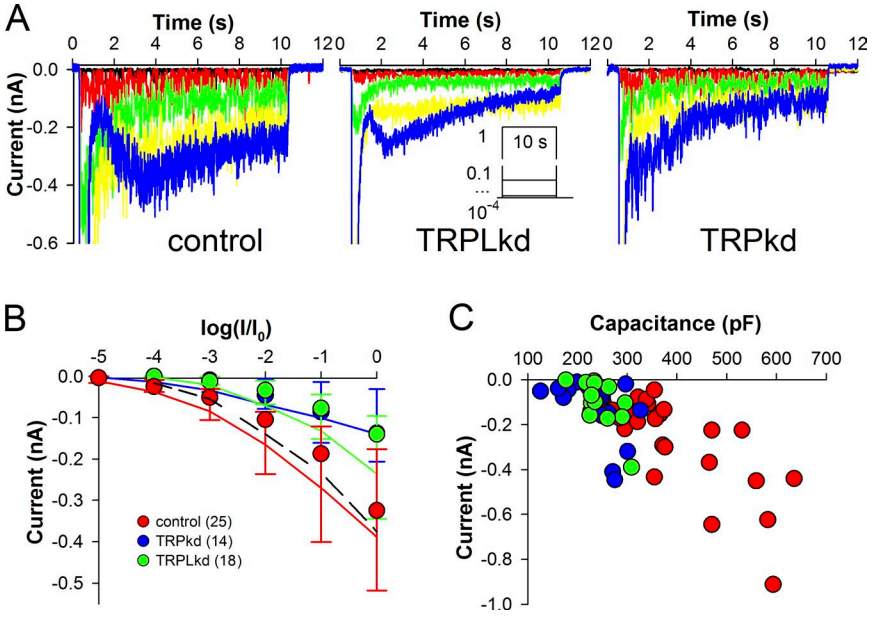

Figure 2. **Macroscopic LICs.** (A) Typical LIC responses of a green-sensitive photoreceptor to 10-s light stimulus of five different intensities, in 10-fold increments, recorded from control, TRPLkd, and TRPkd photoreceptors; inset shows stimulation protocol. (B) Dependence of sustained LIC on light intensity; LIC values were obtained at 5 s after the light onset. Circles show median values, error bars are interquartile ranges (first to third), and solid lines represent mean values. Dashed black line is the sum of mean TRPkd and TRPLkd values. (C) Correlation between photoreceptor capacitance and sustained LIC values obtained at light intensity "−1" as in B; color coding as in B.

for responses produced by the light intensity "−1" (the maximal intensity without pronounced saturation-related phenomena) indicated that control LIC (n = 25) is significantly higher than LIC in TRPkd (n = 18, P = 0.003, MWUT) or TRPLkd (n = 14, P = 0.001, MWUT) photoreceptors. The black dashed trace visualizes the sum of mean LICs in TRPkd and TRPLkd photoreceptors, implying that the knockdown LIC phenotypes might add up. However, it must be considered that the expression of targeted channels is not completely abolished in knockdown photoreceptors and that there might also be compensatory up-regulation of expression of alternative channels (French et al., 2015). Also, there was a correlation between capacitance and LIC amplitude, so that larger photoreceptors generate larger currents: the SROCC values were −0.71 in control (n = 25, P < 10^{-4}), −0.55 in TRPkd (n = 18, P = 0.019), and −0.56 in TRPLkd (n = 14, P = 0.037; Fig. 2 C). These correlations are consistent with data from other species (Frolov et al., 2012; Frolov and Weckström, 2014; Frolov, 2015, 2016).

Kv currents

As described previously, *P. americana* photoreceptors express several distinct Kv currents: a transient IA mediated by Shaker-like channels (Salmela et al., 2012), a slowly activating and inactivating delayed rectifier (IDR) EAG, and a residual noninactivating Kv current possibly related to KCNQ channels (Immonen et al., 2017). In *Drosophila*, transient Shaker and delayed rectifier Shab channels are thought to be expressed in different parts of the photoreceptor (Rogero et al., 1997). Although there is no information on the expression patterns of Kv channels in *P. americana*, moderately positive correlations were reported previously between IDR (but not IA) amplitude and photoreceptor size in *P. americana* (Salmela et al., 2012) as well as in other insect species (Frolov et al., 2012; Frolov and Weckström, 2014; Frolov, 2015). This is consistent with the expression of delayed rectifier channels in close proximity to microvilli, possibly at their bases. We therefore compared IDR in control and knockdown photoreceptors. Fig. 3 A shows a representative Kv current recording from a control photoreceptor. Fig. 3 B compares current–voltage relationships for the mean IDR in control, TRPkd, and TRPLkd photoreceptors. IDR was slightly smaller in TRPLkd photoreceptors (n = 14) than in control (n = 18; p-values range from 0.045 to 0.01 for voltages from −32 to 28 mV, unpaired t test). No other changes in Kv currents were detected.

Voltage responses and bump noise

In intracellular recordings, two light stimuli were used to investigate voltage response properties: a short 3-s steady light stimulus to measure amplitudes of transient and sustained light responses over the entire range of light intensities and a 61-s GWN light contrast to determine IR (see Materials and methods).

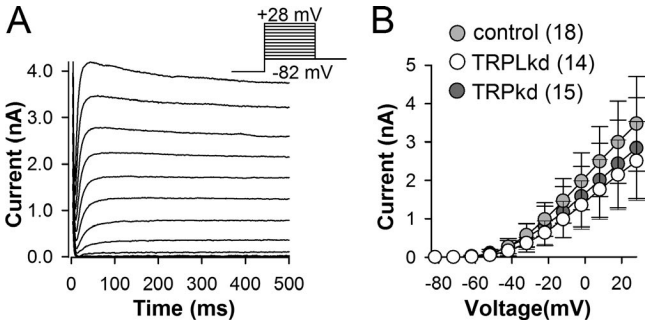

Figure 3. **Kv currents.** (A) Typical Kv currents in control photoreceptor; currents were elicited by 500-ms test pulses from the holding potential of −82 to 28 mV in 10-mV increments; each testing step was preceded by a 1-s prepulse to −102 mV to fully recover the transient IA; the first 3 ms of the current traces containing capacitive transients were removed. (B) Current–voltage relationships for Kv currents in control, TRPLkd, and TRPkd photoreceptors; values are means of the last 100 ms for each trace, and bars denote SD.

Both transient and sustained voltage response amplitudes were smaller in TRPkd and TRPLkd photoreceptors than in control photoreceptors for the entire range of light intensities (Fig. 4 A). Notice that the bump noise is strong in the control and TRPkd photoreceptors, especially at low light intensities, but greatly reduced in the TRPLkd photoreceptors. High bump noise in TRPkd photoreceptors was present even at the brightest light intensities as can be seen from the mean power spectra of bump noise (Fig. 4 B); notice that the data were obtained at the lower intensity "0.3" (as in Fig. 4 C) for control and intensity "1" for knockdown photoreceptors. On average, bump noise was the highest in TRPkd and the lowest in TRPLkd photoreceptors. At 10 Hz, bump noise power magnitude was 0.00146 ± 0.00136 mV^2 in control (n = 12), 0.00141 ± 0.00084 mV^2 in TRPLkd (n = 12), and 0.01697 ± 0.02487 mV^2 in TRPkd (n = 16, P = 0.016, comparison with control, unpaired t test).

Mean light–voltage relationships obtained for peak and sustained depolarizations are shown in Fig. 4 C. Sustained depolarization values represent mean potentials between 2 and 3 s after the onset of light. At the light intensity level corresponding to 0.3 background in Fig. 4 C (red arrow), the sustained depolarization values were 12.2 ± 2.2 mV in control (n = 12), 6.0 ± 3.6 mV in TRPLkd (n = 14, P < 10^{-4}, unpaired t test), and 6.1 ± 3.2 mV (n = 15; P < 10^{-5}, unpaired t test) in TRPkd photoreceptors. The rightward shifts of the light–voltage relationships in TRPkd and TRPLkd photoreceptors relative to control are consistent with the relatively low LICs and absolute sensitivity to light in the knockdowns (Fig. 2).

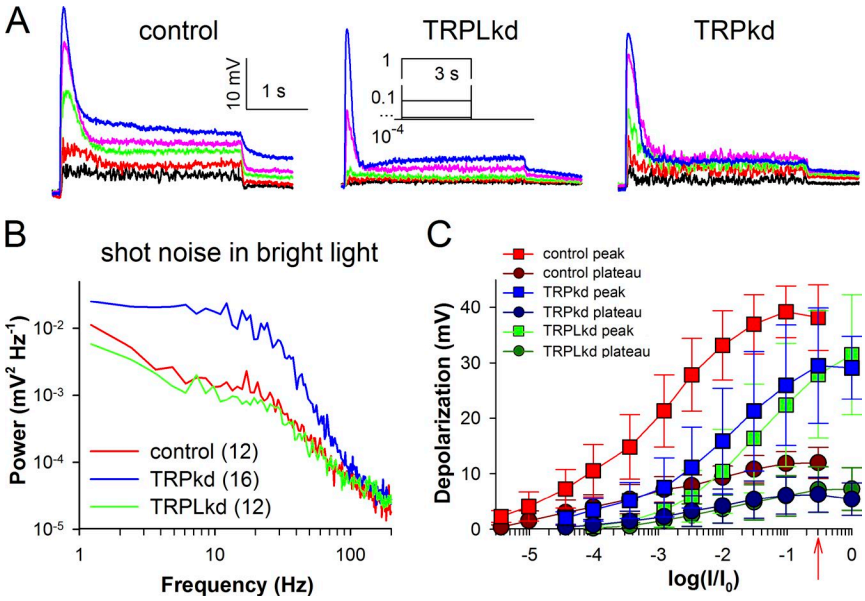

Figure 4. **Voltage responses to light.** (A) Representative responses of control, TRPLkd, and TRPkd photoreceptors to a 3-s steady light stimulus of five different intensities, in 10-fold increments, obtained in intracellular experiments; inset shows stimulation protocol. (B) Mean power spectra of the last 2 s of the 3-s voltage responses to steady light as in A; spectra shown for the brightest light levels, corresponding to intensity "0.3" in C for control and intensity "1" for TRPkd and TRPLkd photoreceptors; error bars are omitted for presentation purposes. (C) Mean dependencies of peak and sustained voltage amplitudes on light intensity. Sustained values were obtained at the end of 3-s responses. Bars denote SD. Red arrow indicates the intensity at which depolarization amplitudes were compared in Results.

Information processing

Fig. 5 A shows examples of voltage responses of a control photoreceptor to GWN stimulation at four backgrounds with light intensity increased in 10-fold increments. Although the GWN stimulus had a relatively low f_{3dB} (50 Hz), it was still three to four times higher than that of a typical response. Therefore, such stimulation should provide ample power in the low frequencies visible to the cockroach.

Unlike in patch-clamp experiments, where ommatidia are exposed to light side-on and IR usually has a clear peak in bright light (Frolov et al., 2012; Frolov and Weckström, 2014; Immonen et al., 2014a; Frolov, 2015), IR in intracellular recordings performed over the same range of light intensities increased gradually in most cases, reaching maximum at the brightest level available (Fig. 5 A, inset). Therefore, IR measurements from the knockdown photoreceptors, which are generally characterized by low sensitivity to light and low plateau depolarization, were exclusively performed at the brightest intensities. Representative gain and signal-to-noise ratio (SNR) functions for control, TRPkd and TRPLkd photoreceptors are shown in Fig. 5 (B and C). To obtain values of maximal gain and f_{3dB}, gain functions were fitted with a first-order Lorentzian function. Gain was substantially higher in control (4.0 ± 1.4 mV per unit of contrast; n = 14) than in TRPLkd (2.0 ± 1.4 mV per unit of contrast; n = 9; P = 0.004), but not in TRPkd (2.8 ± 2.0 mV per unit of contrast; n = 13; P = 0.1). The values of f_{3dB} were 12.1 ± 1.7 Hz in control, 13.7 ± 1.5 in TRPLkd, and 16.6 ± 2.4 in TRPkd (P < 0.003 for comparisons with both control and TRPLkd, unpaired t test) photoreceptors.

IR (IR_{max} for control) positively correlated with membrane depolarization values obtained as means of the last 60 s of responses to the GWN stimulus (Fig. 5 D). The Spearman's ρ was 0.53 in control (n = 14, P = 0.049), 0.73 in TRPkd (n = 13, P = 0.004), and 0.98 in TRPLkd (n = 9, P < 10^{-6}) photoreceptors. The mean IR values for responses in bright light were 52 ± 13 bits/s in control (n = 14), 28 ± 21 bits/s in TRPkd (n = 13, P = 0.0014, unpaired t test, comparison with control), and 54 ± 29 bits/s^1 in TRPLkd (n = 9; P = 0.032, unpaired t test, comparison with TRPkd) photoreceptors (Fig. 5 E).

The finding of high IR in TRPLkd photoreceptors despite their relatively low gain was unexpected and required examination of signal and noise functions, which are shown in Fig. 5 F for control and knockdown photoreceptors. Variability from cell to cell was very high, as can be seen from the inset specifying the median amplitudes and interquartile ranges at the peak frequency of 5 Hz. The median signal power was 0.059 (0.027:0.103) mV^2 in control (n = 14), 0.020 (0.009:0.087) mV^2 in TRPkd (n = 13, P = 0.049, MWUT), and 0.016 (0.002:0.044) mV^2 in TRPLkd (n = 9, P = 0.007, MWUT) photoreceptors. However, although signal functions were fully consistent with the gain functions (Fig. 5 B), noise functions were different, with a much higher noise in TRPkd than in control and with very low noise in TRPLkd photoreceptors. The median values of noise power at 5 Hz were 0.0038 (0.0021:0.0056) mV^2 in control (n = 14), 0.0082 (0.0043:0.0140) mV^2 in TRPkd (n = 13, P = 0.035, MWUT), and 0.0008 (0.0004:0.0012) mV^2 in TRPLkd (n = 9, P = 0.0001, MWUT) photoreceptors. Apparently, these differences between TRPkd and TRPLkd are caused by the differences in bump noise levels (Fig. 4 A).

DISCUSSION

We performed a functional analysis of TRPkd and TRPLkd in *P. americana* photoreceptors. Cockroach reti-

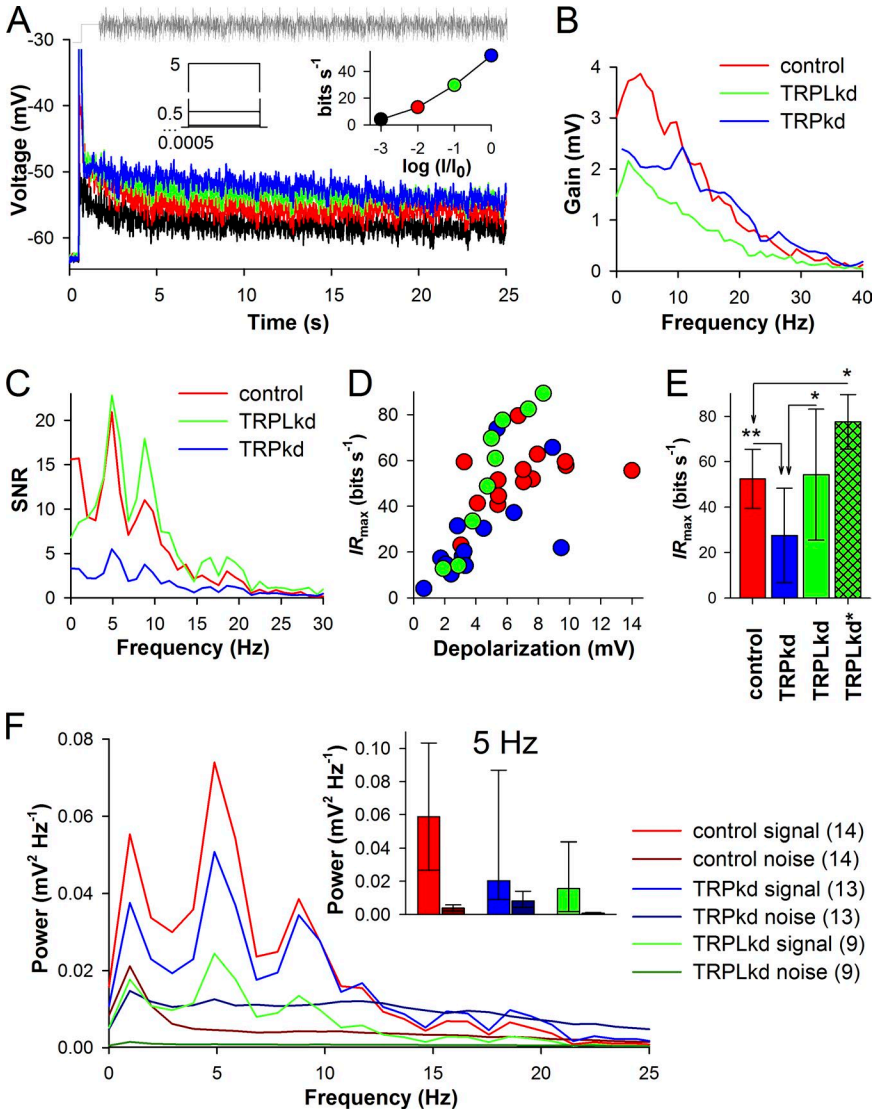

Figure 5. **Signal processing in control, TRPkd, and TRPLkd photoreceptors.** (A) Examples of voltage traces recorded from a control photoreceptor in response to GWN stimulus (gray trace) delivered in 10-fold intensity increments; the first 25 s are shown. Insets show the stimulation protocol and a plot of dependence of IR on light intensity for this photoreceptor; colors correspond to traces. (B and C) Representative gain (B) and SNR (C) functions for responses characterized by maximal IR in each photoreceptor; color coding is the same for B–E. (D) Dependence of IR on depolarization during light response; depolarization values were obtained by averaging plateau voltage during the entire duration of the response except the first second and then subtracting the resting potential and were 6.9 ± 2.9 mV in control, 4.2 ± 2.7 mV in TRPkd, and 5.0 ± 2.0 mV in TRPLkd. (E) The maximal IRs for control, TRPkd, and TRPLkd photoreceptors and a TRPLkd subsample (TRPLkd*) of four photoreceptors characterized by the highest depolarization values (see Discussion for explanation). Bars denote SD. Statistical comparisons were performed using unpaired *t* test; *, 0.05 > P > 0.01; **, P < 0.01. (F) Mean signal and noise functions in the control and knockdown photoreceptors; error bars are omitted for presentation purposes. Inset shows median values of signal and noise amplitudes at 5 Hz; error bars indicate interquartile ranges.

nas were previously shown to have 10 times more TRPL than TRP mRNA, and knockdown of TRPL reduced ERGs efficiently, whereas TRPkd had only a marginal effect (French et al., 2015). This is an important issue, because photoreceptors of the only other species where these channels have been studied in situ, *Drosophila*, express significantly more TRP than TRPL molecules (Bähner et al., 2002). Consequently, *Drosophila trp* knockout mutants display a large functional deficit (Hardie and Minke, 1992), whereas *trpl* knockout mutants are characterized by comparatively subtle changes (Leung et al., 2000).

The observed changes in photoreceptor capacitance and LIC amplitude in knockdowns were unlikely to be caused by nonspecific damage to photoreceptors. First, general cell disruption would probably change mRNA levels for most photoreceptor proteins. However, previous RNAi experiments using the same dsRNA sequences in *P. americana* eyes gave highly specific knockdown of TRP or TRPL mRNA levels without comparable effects on mRNA levels of actin or GAPDH (glyceraldehyde 3-phosphate dehydrogenase, a housekeeping enzyme; French et al., 2015). Second, similar experiments involving RNAi of the EAG gene showed minor, statistically insignificant changes in photoreceptor capacitance and LIC amplitudes (Immonen et al., 2017). However, we cannot be certain that levels of G proteins or other proteins involved in phototransduction cascade that may affect quantum bump size did not change in TRPkd and TRPLkd photoreceptors.

What fraction of targeted channels remained in knocked down photoreceptors? In a previous study, quantitative PCR revealed that ∼10–15% of targeted mRNA remained in the retina after RNAi (French et al., 2015) and about one in eight knockdown cockroaches had normal ERGs. In contrast, in this study, we observed only a few electrophysiologically "normal" photoreceptors in two different knockdown cockroaches, with other photoreceptors in the same retinas showing proper knockdown phenotypes. Considering that in-

trinsic variability in the biophysical properties of *P. americana* photoreceptors is large (Heimonen et al., 2006; Frolov, 2016), such "normal" cells were not excluded from analysis. Consequently, our mean estimates probably include some contribution from photoreceptors that may have been less affected by gene knockdown. This problem is compounded by the possibility of compensatory up-regulation of alternative channel genes (French et al., 2015), which, if reflected in protein expression, would counteract residual contributions of the targeted channel. In the following sections, we discuss key findings of our work.

Light-activated channels and photoreceptor size

What caused the drastic reduction in photoreceptor capacitance? Capacitance measured in whole-cell patch-clamp experiments reflects both light-insensitive membrane and the rhabdom. However, it is unlikely that the rhabdom membrane comprised of tens of thousands of long thin microvilli with small length constants makes a full contribution to the measured capacitance (discussed in Frolov, 2016). Regardless of whether measured capacitance is a true measure of membrane area or an underestimate, the strong correlations between absolute sensitivity and capacitance, as well as between LIC amplitude and capacitance, suggest that a substantial fraction of light-sensitive membrane area could be captured in the estimated capacitance. Therefore, although the observed decrease in capacitance could originate from either light-insensitive membrane, rhabdom, or both, a large reduction in light-insensitive membrane area is unlikely because no photoreceptor had capacitance <140 pF, including three cells from the TRPkd retina that were ∼100-fold less sensitive to light than the least sensitive control photoreceptor (Fig. 1 C).

Similarly, a decrease in rhabdom size could be caused by either a reduction in the number of otherwise unaltered microvilli or by changes in their dimensions. The latter option is unlikely because shorter microvilli, with equal redistribution of the remaining light-activated channels, would cause smaller quantum bumps. This is directly contradicted by our experimental observations: quantum bumps were on average as large in TRPkd photoreceptors as in controls. Therefore, if the numbers of microvilli decreased in knocked down photoreceptors, then light-activated channels must be crucial to the assembly of microvilli, which occurs regularly in many species as a part of the rhabdom renewal cycle (Williams, 1982a,b; Calman and Chamberlain, 1992). This suggests that microvillus formation may require a minimum number of available TRP or TRPL channels.

TRPL channels and information processing

At the resting potential, high-input resistance plus high membrane capacitance forms a low-pass filter with a low corner frequency ($f_{3dB} = 1/2\pi RC$), ∼1–2 Hz in cockroach. Under such conditions, a relatively small quantum bump might fail to elicit a voltage bump large enough to register at the presynaptic terminal, especially considering that cockroach photoreceptors have long axons and the lamina is distant from the retina (Ribi, 1977; Heimonen et al., 2006). As TRPL channels are associated with large quantum bumps, and probably have a much greater unitary conductance than TRP (Reuss et al., 1997), they might be particularly suited for generation of sufficiently large voltage bumps in the dark. The previously reported overexpression of TRPL in light-deprived *Drosophila* with a concomitant increase in photoreceptor sensitivity to light (Bähner et al., 2002) is consistent with this reasoning.

Although large voltage bumps may facilitate transfer of signals in dim light, they will cause high levels of bump noise caused by the stochastic natures of phototransduction and channel opening. This high-gain/high-noise feature of TRPL-mediated responses is evident from Fig. 4 (A and B) and Fig. 5 (B–D). Bump noise decreases with light adaptation as the amplitudes of individual bumps decrease with increasing stimulus intensity. However, exposure of TRPkd photoreceptors to bright light did not reduce noise to control levels (Fig. 4, A and B). Note that the recordings from TRPkd and TRPLkd photoreceptors in Fig. 4 B were performed at generally brighter light than in control (Fig. 4 C). Possible reasons for this lack of bump noise reduction could be a compensatory increase in TRPL expression in TRPkd photoreceptors (French et al., 2015) or altered TRPL properties in the absence of TRP channels, as suggested previously (Leung et al., 2000). Also, if *P. americana* TRPL are suppressed by Ca^{2+} as in *Drosophila* (Reuss et al., 1997), consistent with our previous observations (Immonen et al., 2014b), then knockdown of highly calcium-permeable TRP channels might disrupt bump adaptation and contribute to high levels of bump noise in TRPkd photoreceptors.

Any disadvantage of inherently noisy TRPL channels could be offset by the advantages of high sensitivity in dim environments, where the stochastic nature of photon absorption represents a major source of noise. Under such conditions, vision in *P. americana* is likely to be limited to motion detection without great acuity. Indeed, *P. americana* can distinguish and react to such low-intensity signals that evoke quantum bumps at rates of 0.1/s or less (Honkanen et al., 2014). Furthermore, the deleterious influence of TRPL-linked bump noise on information transfer decreased progressively with increased stimulus intensity in normal photoreceptors (Fig. 4 A, control), although it was not eliminated even in the brightest light (Fig. 5 F).

TRP channels and information processing

Our results indicate that low-noise TRP channels are crucial for information transfer in bright light. It was

previously shown experimentally and by simulation that maximal IRs strongly and positively correlate with the amplitudes of sustained LICs in several species (Frolov et al., 2012; Frolov and Weckström, 2014; Song and Juusola, 2014; Frolov, 2015), with both LIC and IR values similarly correlating with photoreceptor capacitance. These positive correlations have a common cause because photoreceptors with larger rhabdoms (i.e., with more microvilli, which are the information-sampling units) generate larger LICs and transduce input contrasts with higher SNR than photoreceptors with smaller rhabdoms, everything else being equal. Both theory (Laughlin, 1989) and experiment (Heimonen et al., 2012) indicate that LIC is approximately proportional to membrane depolarization.

Although positive correlation between IR and depolarization was not surprising, it has important implications. TRPLkd photoreceptors had the same mean IR as control photoreceptors, despite much smaller LIC and voltage responses. This suggests that if LIC in the cockroach was mediated entirely by TRP instead of TRPL channels, the IR of such photoreceptors would be much higher than in control. The size of improvement can be inferred from Fig. 5 D: if IR values of the four TRPLkd photoreceptors characterized by the largest depolarization were taken separately so that their mean depolarization value were comparable to that in controls, correspondingly 6.7 ± 1.4 and 6.9 ± 2.9 mV, then the mean IR of this subsample (designated as TRPLkd* in Fig. 5 D), 78 ± 12 bits/s, would be significantly higher than 52 ± 13 bits/s in control (P = 0.016, unpaired *t* test). Moreover, this is actually an underestimate because TRPLkd photoreceptors may contain some TRPL channels (French et al., 2015). Therefore, *P. americana* with only TRP channels would probably have superior IR, but at the expense of lower absolute sensitivity and motion detection in very dim light conditions.

Conclusions: Light-activated channels and visual ecology

Accumulating evidence indicates that the two main types of light-activated channels responsible for phototransduction in microvillar photoreceptors, TRP and TRPL, constitute two distinct subsystems specialized for functioning under different illumination conditions: dim versus bright light or, in terms of photoreceptor responses, near the resting potential versus strongly depolarized. We suggest that high-noise, high-gain TRPL channels are crucial for transducing signals in dim light, whereas low-noise, low-gain TRP channels give better information transmission in bright light.

This hypothesis is based on findings in only two insect species. *Drosophila* is a predominantly diurnal fly with small (~60 pF) photoreceptors (Frolov et al., 2016) and with a minor contribution of TRPL channels to LIC, as the TRP to TRPL molecular ratio in rhabdomeral membranes varies from 10:1 in dark-raised flies to 200:1 after prolonged exposure to light (Xu et al., 1997; Paulsen et al., 2000; Bähner et al., 2002). In contrast, *P. americana* TRP and TRPL channels contribute equally to LIC in moderate and bright light, although TRPL seems to play the main role under dim conditions. The IR of *Drosophila* photoreceptors greatly exceeds that of *P. americana*: ~200 bits/s (Juusola and Hardie, 2001) versus 50 bits/s, respectively. As we show here, IR apparently depends on the ion channel composition, so that under otherwise equal conditions, a relative overexpression of TRP channels can be linked to higher IR (Fig. 5 E). Therefore, part of *Drosophila*'s advantage over *P. americana* in IR can probably be explained by the dominant role of TRP channels in the fruit fly. To further test this hypothesis, TRPL/TRP compositions of photoreceptors from other insect species with dissimilar life styles and varying reliance on vision need to be explored. Rapid, diurnal fliers such as blowflies (Paulsen et al., 2000) or dragonflies should express mainly TRP channels, whereas small-eyed nocturnal crawlers should predominantly express TRPL channels.

ACKNOWLEDGMENTS

This research was supported by Natural Sciences and Engineering Research Council of Canada (NSERC) grants RGPIN/5565 (to P.H. Torkkeli) and RGPIN/03712 (to A.S. French).

The authors declare no competing financial interests.

Author contributions: R.V. Frolov conceived the experiments; all authors contributed to the design of experiments; and P. Saari, R.V. Frolov, A.S. French, P.H. Torkkeli, and Hongxia Liu performed experiments. R.V. Frolov analyzed data and wrote the manuscript; all authors discussed findings, provided critical input, edited and approved the manuscript, and agree to be accountable for all aspects of the work. All persons designated as authors qualify for authorship, and all those who qualify for authorship are listed.

Angus C. Nairn served as editor.

Submitted: 10 December 2016
Accepted: 6 February 2017

REFERENCES

Bähner, M., S. Frechter, N. Da Silva, B. Minke, R. Paulsen, and A. Huber. 2002. Light-regulated subcellular translocation of *Drosophila* TRPL channels induces long-term adaptation and modifies the light-induced current. *Neuron.* 34:83–93. http://dx.doi.org/10.1016/S0896-6273(02)00630-X

Calman, B.G., and S.C. Chamberlain. 1992. Localization of actin filaments and microtubules in the cells of the *Limulus* lateral and ventral eyes. *Vis. Neurosci.* 9:365–375. http://dx.doi.org/10.1017/S0952523800010774

French, A.S., S. Meisner, H. Liu, M. Weckström, and P.H. Torkkeli. 2015. Transcriptome analysis and RNA interference of cockroach phototransduction indicate three opsins and suggest a major role for TRPL channels. *Front. Physiol.* 6:207. http://dx.doi.org/10.3389/fphys.2015.00207

Frolov, R.V. 2015. Biophysical properties of photoreceptors in Corixa punctata facilitate diurnal life-style. *Vision Res.* 111:75–81. http://dx.doi.org/10.1016/j.visres.2015.03.026

Frolov, R.V. 2016. Current advances in invertebrate vision: Insights from patch-clamp studies of photoreceptors in apposition eyes. *J. Neurophysiol.* 116:709–723. http://dx.doi.org/10.1152/jn.00288.2016

Frolov, R., and M. Weckström. 2014. Developmental changes in biophysical properties of photoreceptors in the common water strider (*Gerris lacustris*): Better performance at higher cost. *J. Neurophysiol.* 112:913–922. http://dx.doi.org/10.1152/jn.00239.2014

Frolov, R., E.V. Immonen, M. Vähäsöyrinki, and M. Weckström. 2012. Postembryonic developmental changes in photoreceptors of the stick insect *Carausius morosus* enhance the shift to an adult nocturnal life-style. *J. Neurosci.* 32:16821–16831. http://dx.doi.org/10.1523/JNEUROSCI.2612-12.2012

Frolov, R., E.V. Immonen, and M. Weckström. 2016. Visual ecology and potassium conductances of insect photoreceptors. *J. Neurophysiol.* 115:2147–2157. http://dx.doi.org/10.1152/jn.00795.2015

Hardie, R.C. 2014. Photosensitive TRPs. *Handb. Exp. Pharmacol.* 223:795–826. http://dx.doi.org/10.1007/978-3-319-05161-1_4

Hardie, R.C., and B. Minke. 1992. The trp gene is essential for a light-activated Ca^{2+} channel in *Drosophila* photoreceptors. *Neuron.* 8:643–651. http://dx.doi.org/10.1016/0896-6273(92)90086-S

Heimonen, K., I. Salmela, P. Kontiokari, and M. Weckström. 2006. Large functional variability in cockroach photoreceptors: Optimization to low light levels. *J. Neurosci.* 26:13454–13462. http://dx.doi.org/10.1523/JNEUROSCI.3767-06.2006

Heimonen, K., E.V. Immonen, R.V. Frolov, I. Salmela, M. Juusola, M. Vähäsöyrinki, and M. Weckström. 2012. Signal coding in cockroach photoreceptors is tuned to dim environments. *J. Neurophysiol.* 108:2641–2652. http://dx.doi.org/10.1152/jn.00588.2012

Honkanen, A., J. Takalo, K. Heimonen, M. Vähäsöyrinki, and M. Weckström. 2014. Cockroach optomotor responses below single photon level. *J. Exp. Biol.* 217:4262–4268. http://dx.doi.org/10.1242/jeb.112425

Immonen, E.V., I. Ignatova, A. Gislen, E. Warrant, M. Vähäsöyrinki, M. Weckström, and R. Frolov. 2014a. Large variation among photoreceptors as the basis of visual flexibility in the common backswimmer. *Proc. Biol. Sci.* 281:20141177. http://dx.doi.org/10.1098/rspb.2014.1177

Immonen, E.V., S. Krause, Y. Krause, R. Frolov, M.T. Vähäsöyrinki, and M. Weckström. 2014b. Elementary and macroscopic light-induced currents and their Ca^{2+}-dependence in the photoreceptors of *Periplaneta americana*. *Front. Physiol.* 5:153. http://dx.doi.org/10.3389/fphys.2014.00153

Immonen, E.-V., A.S. French, P.H. Torkkeli, H. Liu, M. Vähäsöyrinki, and R.V. Frolov. 2017. EAG channels expressed in microvillar photoreceptors are unsuited to diurnal vision. *J. Physiol.* http://dx.doi.org/10.1113/JP273612

Juusola, M., and R.C. Hardie. 2001. Light adaptation in *Drosophila* photoreceptors: I. Response dynamics and signaling efficiency at 25 degrees C. *J. Gen. Physiol.* 117:3–25 (publishd erratum appears in *J. Gen. Physiol.* 2001. 117:3). http://dx.doi.org/10.1085/jgp.117.1.3

Laughlin, S.B. 1989. The role of sensory adaptation in the retina. *J. Exp. Biol.* 146:39–62.

Leung, H.T., C. Geng, and W.L. Pak. 2000. Phenotypes of trpl mutants and interactions between the transient receptor potential (TRP) and TRP-like channels in *Drosophila*. *J. Neurosci.* 20:6797–6803.

Montell, C., and G.M. Rubin. 1989. Molecular characterization of the *Drosophila trp* locus: A putative integral membrane protein required for phototransduction. *Neuron.* 2:1313–1323. http://dx.doi.org/10.1016/0896-6273(89)90069-X

Niemeyer, B.A., E. Suzuki, K. Scott, K. Jalink, and C.S. Zuker. 1996. The *Drosophila* light-activated conductance is composed of the two channels TRP and TRPL. *Cell.* 85:651–659. http://dx.doi.org/10.1016/S0092-8674(00)81232-5

Paulsen, R., M. Bahner, and A. Huber. 2000. The PDZ assembled "transducisome" of microvillar photoreceptors: The TRP/TRPL problem. *Pflugers Arch.* 439:r181–r183. http://dx.doi.org/10.1007/s004240000138

Phillips, A.M., A. Bull, and L.E. Kelly. 1992. Identification of a *Drosophila* gene encoding a calmodulin-binding protein with homology to the trp phototransduction gene. *Neuron.* 8:631–642. http://dx.doi.org/10.1016/0896-6273(92)90085-R

Reuss, H., M.H. Mojet, S. Chyb, and R.C. Hardie. 1997. In vivo analysis of the *Drosophila* light-sensitive channels, TRP and TRPL. *Neuron.* 19:1249–1259. http://dx.doi.org/10.1016/S0896-6273(00)80416-X

Ribi, W.A. 1977. Fine structure of the first optic ganglion (lamina) of the cockroach, *Periplaneta americana*. *Tissue Cell.* 9:57–72. http://dx.doi.org/10.1016/0040-8166(77)90049-0

Rogero, O., B. Hämmerle, and F.J. Tejedor. 1997. Diverse expression and distribution of Shaker potassium channels during the development of the *Drosophila* nervous system. *J. Neurosci.* 17:5108–5118.

Salmela, I., E.V. Immonen, R. Frolov, S. Krause, Y. Krause, M. Vähäsöyrinki, and M. Weckström. 2012. Cellular elements for seeing in the dark: Voltage-dependent conductances in cockroach photoreceptors. *BMC Neurosci.* 13:93. http://dx.doi.org/10.1186/1471-2202-13-93

Song, Z., and M. Juusola. 2014. Refractory sampling links efficiency and costs of sensory encoding to stimulus statistics. *J. Neurosci.* 34:7216–7237. http://dx.doi.org/10.1523/JNEUROSCI.4463-13.2014

Williams, D.S. 1982a. Ommatidial structure in relation to turnover of photoreceptor membrane in the locust. *Cell Tissue Res.* 225:595–617. http://dx.doi.org/10.1007/BF00214807

Williams, D.S. 1982b. Rhabdom size and photoreceptor membrane turnover in a muscoid fly. *Cell Tissue Res.* 226:629–639. http://dx.doi.org/10.1007/BF00214790

Xu, X.Z., H.S. Li, W.B. Guggino, and C. Montell. 1997. Coassembly of TRP and TRPL produces a distinct store-operated conductance. *Cell.* 89:1155–1164. http://dx.doi.org/10.1016/S0092-8674(00)80302-5